**INTEGRATING CRISM AND TES HYPERSPECTRAL DATA TO CHARACTERIZE A MASSIVE KAOLIN-GROUP MINERAL DEPOSIT IN KASHIRA CRATER, MARS.** T. A. Goudge[1], J. F. Mustard[1], J. W. Head[1], and M. R. Salvatore[1], [1]Dept. of Geological Sciences, Box 1846, Brown University, Providence, RI 02912. (Contact: Tim_Goudge@brown.edu)

**Introduction:** Kashira crater is an ~60 km diameter, heavily degraded crater in the Margaritifer Terra region of Mars. Kashira has a volcanically resurfaced floor (VRF) [1,2] and is host to a massive, ~480 km$^2$, light-toned mound deposit (LTM) that has previously been shown to be kaolin-group mineral (e.g., kaolinite, halloysite, dickite) bearing [1,3] (**Figure 1**). Kashira crater also has both an inlet and outlet valley that cut the crater rim, and so the crater was once an open-basin lake [4], prior to being volcanically resurfaced at ~3.66 Ga [2].

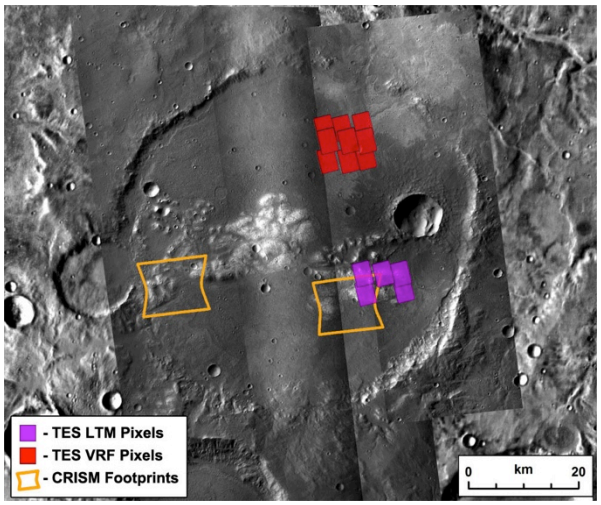


**Figure 1:** *Kashira crater overview. North is up. Note the two light-toned mound deposits and the smooth, volcanically resurfaced floor [1,2]. Approximate locations of LTM and VRF TES pixels are indicated in purple and red respectively, and CRISM observation footprints are outlined in orange. Mosaic of CTX [5] images B01_010091_1541, B02_010447_1528, B04_011370_1532 and B05_011581_1521 overlain on the ~100 m/pixel global THEMIS daytime IR mosaic [6].*

The size and composition of the LTM offers a unique site to study an ancient martian alteration mineral deposit using multiple remote sensing datasets, primarily from the Compact Reconnaissance Imaging Spectrometer for Mars (CRISM) [7] and the Thermal Emission Spectrometer (TES) [8] instruments. Previous studies of aqueous alteration minerals on Mars using CRISM data have primarily focused on the detection and presence/absence of different alteration minerals based on the strength, shape and position of overtone and combination tone absorptions associated with bound OH and $H_2O$ within silicate and sulfate mineral structures [e.g., 1,3,9-12]. While such detections have been very important in helping constrain the aqueous history of Mars [e.g., 3,9-12], the question of alteration mineral abundance has been left largely unaddressed by analyses of CRISM data, although it has been addressed for some regions with OMEGA data [e.g., 13]. The goal of this study is to use both visible-near infrared (VNIR), i.e. CRISM, and thermal infrared (TIR), i.e. TES, data to characterize the mineralogy of the LTM unit, focusing on the quantification of the abundance of the kaolin-group mineral. The high-spatial resolution CRISM data is widely used to positively detect hydrated minerals [e.g., 3,9-12], while the low-spatial resolution TES data is commonly used to determine modal mineralogy [e.g., 14-17], and so integrating these two datasets will offer a unique perspective of the martian surface.

**Methods:** *TES.* The bulk mineralogies of the LTM and VRF units were investigated using data from the low-spatial, high-spectral resolution TES instrument. TES is a TIR spectrometer that covers the wavelength range of ~6-50 μm (~200-1650 cm$^{-1}$), with an average pixel size of ~3 x 6 km [8]. Only high quality TES data (surface temperature >260 K, emission angle <10°, low dust and ice opacities, and from early in the mission, i.e. OCK <7000) were used in this analysis, resulting in 5 pixels across the LTM and 9 across the VRF (**Figure 1**).

To assess the modal mineralogy of the two surface units, the TES spectra were linearly unmixed using the methods of [14], an approach commonly used to estimate modal mineralogy from TES data [e.g., 15-17]. A spectral endmember library similar to that of [17] was used, and contains 48 minerals, including 12 phyllosilicates and 4 kaolin-group minerals, plus 6 atmospheric components. The total error on each fit was calculated as a root-mean-square error (RMSE), and the error on each output endmember abundance was calculated from a covariance matrix of endmember coefficients [18].

To supplement the standard linear unmixing, we have developed a method for iterative fitting of TES spectra that acts as a sensitivity analysis for various endmember components. This iterative fitting method operates by randomly varying the secondary minerals (e.g., phyllosilicates, evaporites) included in the endmember library for linear unmixing to see what range of mineral mixtures result in a fit with an acceptable level of error (i.e., RMSE <0.003).

*CRISM.* The mineralogy of the LTM was also studied using two CRISM targeted images located over both the eastern and western portions of the mound (**Figure 1**). CRISM is a VNIR hyperspectral imaging spectrometer that covers the wavelength range of ~0.36-3.9 μm at a spatial resolution of ~18 m/pixel (full-resolution targeted images) [7].

Here, we present preliminary results of the non-linear spectral unmixing of CRISM data using the Hapke radiative transfer model [19,20]. The approach taken here is to model a spectrum of the LTM as a four component mixture using three endmembers derived from within the same CRISM scene in addition to a library spectrum of a kaolin-group mineral [21] across the wavelength range of ~1-2.6 μm. CRISM I/F spectra and library reflectance spectra were converted to single scattering albedo (*w*), a material spectral property that sums linearly based on the areal proportion of that material in an intimate mixture, using the Hapke model [18]. Once converted to *w*, the best fit (i.e., lowest RMSE) mixture of the four endmembers to the LTM spectrum was determined, and the corresponding abundances output.

**Results:** *TES.* Results from the standard linear unmixing of the LTM (**Figure 2**) indicate a kaolin-group mineral component of ~32% (±~10%), with additional components of pyroxene and plagioclase. The VRF unmixing suggests that it is primarily dominated by plagioclase and low-Ca pyroxene, consistent with previous CRISM results [2]. Results from the sensitivity analysis show that a kaolin-group mineral is detected within the LTM at a robust level (i.e., at >10%) in ~98.7% of the 10,000 trial runs with an average modeled abundance of ~29% (standard deviation = ~8%).

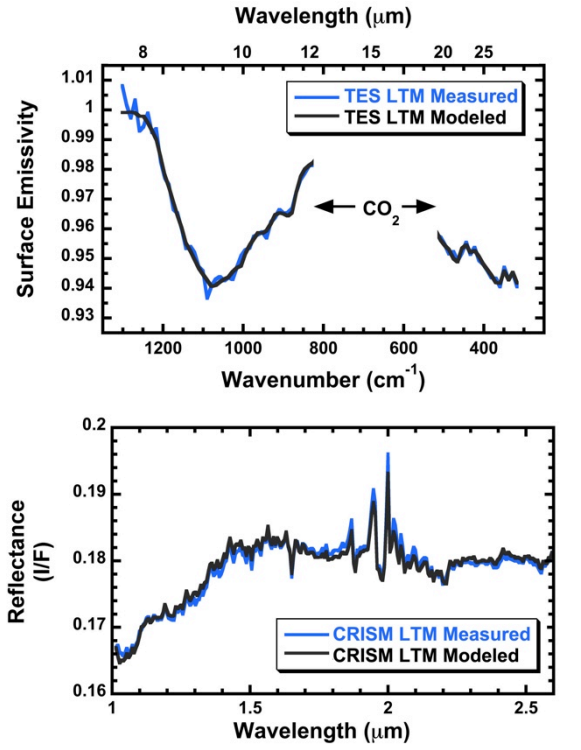


**Figure 2:** *Model output results for the LTM for TES linear unmixing (top plot) and CRISM non-linear unmixing (bottom plot). Both plots show the LTM 'measured' spectrum (i.e., the extracted spectrum from TES and CRISM over the LTM) in blue and the modeled spectrum in black.*

*CRISM.* Results of the CRISM non-linear unmixing (**Figure 2**) suggest that the LTM is best modeled by a combination of the geologic units within the CRISM scene (primarily the VRF and a low-albedo, dusty terrain) with the addition of ~13-15% of a kaolin-group mineral, with the precise abundance dependent on the specific kaolin-group mineral used and which CRISM scene is used (all model outputs have RMSE <0.003).

**Discussion:** Based on the results presented above, we suggest that the LTM within Kashira crater has an appreciable component of a kaolin-group mineral, likely to be on the order of tens of volume percent of the deposit. The TES and CRISM results agree well to a first-order, although there is a slight discrepancy between the two modeled abundances. One potential source for the disparity in the model outputs is the fact that the endmembers used in the CRISM analysis are in-scene derived units plus a kaolin-group mineral, while the endmembers for the TES analysis are largely pure mineral phases. Although there is this slight difference in the modeled abundance of the kaolin-group mineral from the TES and CRISM unmixing results, we believe that our analyses have successfully integrated the TES and CRISM datasets at this site to achieve two estimates of quantitative mineralogy that are in good agreement.

Future work will focus on potential formation mechanisms of the LTM within Kashira crater, and the implications of the modal mineralogy results presented here. Of particular interest in such work is the obvious difference in geologic setting between this deposit and other kaolin-group mineral deposits that have been observed on the surface of Mars, such as Nili Fossae and Mawrth Vallis, where the kaolin-group mineral is observed in a distinct stratigraphy above Fe/Mg-smectite [e.g., 9-12]. We are also working on assessing the spatial distribution of the kaolin-group mineral within the LTM using a variety of spectral unmixing techniques for entire CRISM image cubes.

**References:** [1] Goudge, T., et al. (2012), *Icarus*, **219**:211. [2] Goudge, T., et al. (2012), *JGR*, **117**:E00J21. [3] Wray, J., et al. (2009), *Geology*, **37**:1043. [4] Fassett, C. and Head, J. (2008), *Icarus*, **198**:37. [5] Malin, M., et al. (2007), *JGR,* **112**:E05S04. [6] Christensen, P., et al. (2004), *Space Sci. Rev.*, **110**:85. [7] Murchie, S., et al. (2007), *JGR,* **112**:E05S03. [8] Christensen, P., et al. (2001), *JGR*, **106**:23,823. [9] Mustard, J., et al. (2008), *Nature*, **454**:305. [10] Ehlmann, B., et al. (2009), *JGR*, **114**:E00D08. [11] Murchie, S., et al. (2009), *JGR*, **114**:E00D06. [12] Ehlmann, B., et al. (2011), *Nature*, **479**:53. [13] Poulet, F., et al. (2008), *Astron. Astrophys.*, **487**:L41. [14] Ramsey, M. and Christensen, P. (1998), *JGR*, **103**:577. [15] Bandfield, J., et al. (2000), *Science*, **287**:1626. [16] Bandfield, J. (2002), *JGR,* **107**:E6,5042. [17] Rogers, A. and Christensen, P. (2007), *JGR*, **112**:E01003. [18] Rogers, A. and Aharonson, O. (2008), *JGR*, **113**:E06S14. [19] Hapke, B. (1981), *JGR*, **86**:3039. [20] Hapke, B. (2002), *Icarus*, **157**:523. [21] CRISM Spectral Library (2006), *PDS Geosci. Node*, <http://pds-geosciences.wustl.edu/missions/mro/spectral_library.htm>. [22] Malin, M. and Edgett, K. (2000), *Science*, **290**:1927. [23] Milliken, R., et al. (2010), *GRL*, **37**:L04201.